Interfacial Tension in Binary Polymer Blends in the Presence of Block Copolymers. 2. Effects of Additive Architecture and Composition

H. Retsos[†] and S. H. Anastasiadis*

Institute of Electronic Structure and Laser, Foundation for Research and Technology−Hellas, P.O. Box 1527, 711 10 Heraklion, Crete, Greece, and Department of Physics, University of Crete, 710 03 Heraklion, Crete, Greece

S. Pispas[‡] and J. W. Mays[§]

Department of Chemistry, University of Alabama at Birmingham, Birmingham, Alabama 35294

N. Hadjichristidis

Department of Chemistry, University of Athens, Zografou University City, 157 01 Zografou, Athens, Greece

Received September 29, 2003; Revised Manuscript Received November 2, 2003

ABSTRACT: The effect of the macromolecular architecture and composition of block copolymer additives on the reduction of the interfacial tension between two immiscible homopolymers is investigated. A series of (polyisoprene)$_2$(polystyrene), I_2S, graft copolymers with constant molecular weight and varying composition are utilized as additives in polystyrene/polyisoprene blends. The interfacial tension decreases with the addition of small amounts of copolymer and reaches a plateau at higher copolymer concentration. The interfacial tension at interfacial saturation depends on copolymer composition exhibiting a minimum, which is lower than that using a symmetric diblock with the same molecular weight. Moreover, the interfacial tension at saturation depends on the side of the interface the copolymer is introduced; adding it to the polyisoprene phase is much more efficient than adding it to polystyrene. This is due to the asymmetric architecture of the copolymer and points to the fact that a local equilibrium can only be attained in such systems: the copolymer reaching the interface from one homopolymer phase probably does not diffuse to the other phase. The fact that this behavior is not a kinetic effect is verified using (polystyrene)$_2$(polyisoprene), S_2I, grafts, which show the mirror image behavior. The effectiveness of the interfacial modifiers is, thus, controlled by the unfavorable interactions, which drive the additive toward the interface, and the possibility of micelle formation, which hinders its activity.

I. Introduction

Mixing two or more components with complementary properties is largely utilized to improve the performance of polymeric materials for many important industrial applications. Suitably chosen block or graft copolymers are widely used in immiscible polymer blends as compatibilizers for controlling the morphology (phase structure) and the interfacial adhesion between the phases to obtain an optimized product.[1] This is due to their interfacial activity, i.e., to their affinity to selectively segregate to the interface between the phase-separated homopolymers,[2−4] which reduces the interfacial tension between the two macrophases,[5−8] prevents coalescence[9,10] (thus leading to a finer and more homogeneous dispersion during mixing[9,11]), and enhances interfacial adhesion.[12]

The effectiveness of block or graft copolymers as emulsifiers is determined by their partitioning to the blend interface,[2,3] where each block preferentially extends into its respective homopolymer phase.[4,13−15] The tendency for interfacial migration is predicted to depend on the molecular weights of the copolymer blocks relative to those of the homopolymers,[13,16−19] on the interaction parameter balance between the homopolymers and the copolymer blocks,[20] and on the macromolecular architecture/topology and composition of the copolymers.[11b,21−26]

There are a few points, however, which are usually overlooked especially in theoretical treatments. One relates to the fact that mixing the additive with one of the components may lead to the formation of copolymeric micelles in the homopolymer matrix.[27] These would compete with the interfacial region for copolymer chains, and the amount of copolymer at the interface or in micelles would depend on the relative reduction in the free energy; typically, much of the premade copolymer would reside in micelles for high molecular weight additives. The effect of the existence of micelles on the interfacial partitioning of diblock copolymers at the polymer/polymer interface has received little attention.[3,16−18,28−31] As an alternative, in situ formation of copolymers (usually grafts) is utilized[9,32,33] to overcome the "wasting" of the additive into micelles. The second point relates to the possible trapping[14] of copolymer chains at the interface, which leads to partial equilibrium situations. Finally, since in a typical preparation of homopolymer/copolymer blends the system may be diffusion-controlled, the optimal conditions for the molecular design of interfacially active copolymers obtained from equilibrium considerations may have to be modified.

* To whom correspondence should be addressed. E-mail: spiros@iesl.forth.gr.
[†] Present address: Institut de Biologie Structurale, 41 rue Jules Horowitz, 38027 Grenoble, France.
[‡] Present address: Department of Chemistry, University of Athens, 157 01 Zografou, Athens, Greece.
[§] Present address: Department of Chemistry, University of Tennessee, Knoxville, TN 37996-1600.

10.1021/ma035463e CCC: $27.50
Published on Web 12/23/2003

In a recent paper[30] an investigation was presented on the effect of the molecular weight (MW) and concentration (ϕ_{add}) of compositionally symmetric diblock copolymer additives on the interfacial tension between two immiscible homopolymers. The observed dependence of the interfacial tension on the additive concentration agreed with previous investigations: a sharp decrease with addition of a small amount of copolymer followed by a leveling off at higher copolymer concentrations. However, the reduction of the interfacial tension was a nonmonotonic function of the copolymer additive molecular weight at constant copolymer concentration in the plateau region. The emulsifying effect, $\Delta\gamma = \gamma_0 - \gamma$, increased by increasing the additive MW for low MWs, whereas it decreased by further increasing the copolymer MW, thus going through a maximum. This was understood by considering the possibility of micelle formation as the additive MW increased, leading to a three-state equilibrium among copolymer chains adsorbed at the interface, chains homogeneously mixed with the bulk homopolymers, and copolymer chains at micelles within the bulk phases; a simple model qualitatively showed a similar behavior. The presence of micelles for high MW additives and their absence for low MWs was supported by small-angle X-ray scattering data.

In the present paper, the earlier work is extended by investigating the effect of the macromolecular architecture and composition (f) of block copolymer additives on the interfacial tension between two immiscible homopolymers; the investigation is performed using a technique based on the analysis of axisymmetric pendant fluid drop profiles.[5,30,34] The systems investigated are polystyrene/polyisoprene blends in the presence of (polyisoprene)$_2$(polystyrene), I_2S, and (polystyrene)$_2$(polyisoprene), S_2I, graft copolymers; the series of grafts utilized possess constant molecular weight and varying composition. A decrease in interfacial tension is observed with addition of small amounts of copolymer followed by a leveling off (plateau) as the copolymer concentration (ϕ_{add}) increases, illustrating the surfactant-like behavior of the graft copolymers. The interfacial tension at interfacial saturation (plateau regime) is a nonmonotonic function of the copolymer composition f exhibiting a minimum versus f, whereas it is lower than that for a symmetric diblock with the same total molecular weight. The dependence on f can be understood as a competition between the decreased affinity of the copolymer within the homopolymer phase when the size of the "other" constituent increases, which increases the driving force of the copolymer toward the interface, and the possibility of micellar formation. These ideas are supported by small-angle X-ray scattering measurements, which indicate the formation or absence of micelles. Furthermore, an important finding is that the final interfacial tension at saturation depends on the side of the interface the I_2S graft copolymer is added: when the I_2S is added to the polyisoprene side, the interfacial tension reduction is more significant; i.e., the interfacial activity of the additive is higher. This points to a local equilibrium that is only attained in such systems: the copolymer reaching the interface from one homopolymer phase does not diffuse to the other phase. When using the respective S_2I graft copolymers, a mirror image behavior is obtained; i.e., addition of the S_2I graft to the polystyrene side follows the behavior of the I_2S added to polystyrene and vice versa; this signifies that this behavior is not a kinetic effect but rather is due to a trapping of the system to a stationary state of local equilibrium.

The remainder of this paper is arranged as follows: Following the Experimental Section (section II), the results of the interfacial tension investigations are presented in section III and are discussed in relation to a theoretical attempt to predict the behavior. The concluding remarks constitute section IV.

Table 1. Molecular Characteristics of the (Polyisoprene)$_2$(polystyrene) and (Polyisoprene)(polystyrene)$_2$ Graft Copolymers

species	M_w	M_w/M_n	w_{PS}[a]	N[b]	f_{PI}[c]	ref
I_2S-1	106000	1.04	0.91	1191	0.10	36
I_2S-2	90800	1.04	0.84	1031	0.18	36
I_2S-3	87400	1.04	0.67	1017	0.36	36
I_2S-4	92000	1.04	0.49	1098	0.54	36
I_2S-5	89800	1.04	0.35	1093	0.68	36
I_2S-6	101000	1.04	0.20	1254	0.82	36
I_2S-7	91300	1.06	0.10	1149	0.91	36
S_2I-4	93000	1.06	0.48	1112	0.53	37
SI	96000	1.08	0.61	1127	0.59	30, 36
PS	9860	1.05	1.00	112	1.00	30
PI	4000	1.06	0.00	81	0.00	30

[a] Polystyrene weight fraction by SEC−UV. [b] Number of copolymer segments based on average segmental volume. [c] Polyisoprene volume fraction.

II. Experimental Section

Materials. A series of I_2S three-miktoarm star copolymers (simple grafts) were synthesized by anionic polymerization using high-vacuum techniques in glass reactors provided with break seals for the addition of reagents and constrictions for removal of products; the controlled chlorosilane chemistry approach was utilized. Details on the synthesis and characterization of these systems have been described previously.[35−37] The monomers (styrene, isoprene), the solvent (benzene), and the linking agent (methyltrichlorosilane) were purified to the standards required for high-vacuum techniques, following well-known procedures.[38] Living polystyrenyllithium [(PS)Li] and polyisoprenyllithium [(PI)Li] precursors were synthesized in benzene using *sec*-butyllithium initiator. A ~3% w/v solution of (PS)Li in benzene was allowed to react with a large excess (SiCl/Li = 100) of methyltrichlorosilane (CH_3SiCl_3) to produce (PS)Si(CH_3)Cl_2, followed by the removal of the unreacted CH_3SiCl_3 and benzene on the vacuum line. Next, an excess of (PI)Li in benzene was added to a benzene solution of the macromolecular difunctional linking agent, (PS)Si(CH_3)Cl_2, to obtain the CH_3Si(PS)(PI)$_2$ three-miktoarm star copolymers I_2S. The excess (PI)Li was deactivated with degassed methanol. The same procedure was utilized for the synthesis of S_2I three-miktoarm star copolymers where the first step involved the incorporation of the polyisoprene arm (adding (PI)Li) and the second that of the two polystyrene arms (adding an excess of (PS)Li). The desired I_2S or S_2I three-arm star was isolated from the reaction mixture by solvent/nonsolvent fractionation. The fractionated final products were rigorously characterized by size exclusion chromatography (SEC) with both RI and UV detectors, membrane osmometry, low-angle laser light scattering, and ^{1}H NMR to provide the molecular characteristics of the materials. The microstructure of the dienic sequences was analyzed by ^{1}H and ^{13}C NMR spectroscopy to be ca. 90% 1,4 and ca. 10% 3,4. The molecular characteristics of the samples are given in Table 1. All samples have approximately the same overall molecular weight and varying compositions. Note that in the I_2S samples the polystyrene sequence is perdeuterated (d_8-styrene).

A polystyrene-*block*-polyisoprene diblock copolymer, SI, was synthesized under high vacuum in a glass-sealed apparatus at room temperature using benzene as the solvent and *s*-BuLi as the initiator, with styrene being polymerized first.[30,36c] After the completion of the reaction for both blocks, the living ends

were neutralized with degassed methanol. The copolymer's molecular characteristics obtained as before are given in Table 1.

The polyisoprene (PI) homopolymer was synthesized anionically under an argon atmosphere by K. Hong and kindly provided to us. The polystyrene (PS) homopolymer (Polymer Laboratories, Ltd.) was used in this study as received. The characteristics of the PS and PI homopolymers are also shown in Table 1.

Interfacial Tension Measurements. The interfacial tension between the two different phases (with or without the additive) was measured with the pendant drop method using a technique based on the analysis of axisymmetric fluid drop profiles.[5,30,34] Because of the high viscosities and the viscoelastic character of polymeric materials, equilibrium static techniques, such as drop profile methods, are better suited for measuring surface/interfacial tensions; the pendant/sessile drop method has been proven to be the most versatile in that respect (a comparison between different techniques was recently presented[39]). The method is based on the principle that the shape of the profile of a drop of one fluid into a matrix of another is governed by a force balance between interfacial tension and gravity forces, which is described by the Bashforth−Adams equation.[40] The shape is controlled by the shape parameter $B = ac^{1/2} = a[g\Delta\rho/\gamma]^{1/2}$, where a is the radius of curvature at the drop apex, g is the gravitational constant, γ is the interfacial tension, $\Delta\rho$ is the density difference across the interface, and $c = g\Delta\rho/\gamma$.

The pendant drop is formed in a heated cell with temperature control up to 300 °C with accuracy ±1 °C. The optical system includes a motorized zoom lens with the highest magnification such that a 1 mm subject at distance 10 cm covers an 11 in. screen of the video monitor. The video image of the drop is digitized by an AT&T Targa frame grabber resident within a microcomputer.[41] The resulting image is processed using global thresholding and near-neighbor analysis to extract the experimental drop profile. This profile is then analyzed with a robust shape comparison algorithm, which utilizes the repeated median concept that reduces the five-variable optimization (usually needed for shape comparison) to a single-variable search of the shape parameter B (the other parameters can be calculated independently[34]). The interfacial tension, γ, is calculated from the value of the magnification at the best-fit value of B, τ^*, since $\tau^* = 1/(c^*)^{1/2} = [\gamma/(g\Delta\rho)]^{1/2}$. Utilizing the magnification factor τ^* that corresponds to the optimum B value and knowing the densities of the drop and the matrix phase allow calculation of the interfacial tension γ. The step-by-step performance of the routine for the analysis of the profile of a typical drop of PS in the matrix of PI at 140 ± 1 °C has been presented in an earlier publication.[30]

The copolymers are premixed at certain concentrations with either the PS or the PI homopolymer in toluene followed by slow evaporation of the solvent. Fluid drops of either pure PS or the PS mixtures are then formed at the tip of a glass capillary tube of a Drummond positive displacement syringe in a fluid matrix of the pure PI or of the PI mixture phase. In the majority of previous studies, the copolymer was preblended with the dispersed phase to control more precisely the amount that could diffuse to the interface and to minimize the distance traveled by the copolymer molecules to reach the polymer/polymer interface.[6] This preblending procedure has been adopted before not only for interfacial tension studies[5−7,30] but also for the preparation of specimens for transmission electron microscopy experiments.[2a,11b] For symmetric diblock copolymer additives, it was expected and found that, at equilibrium, the resulting interfacial tension is insensitive to whether the additive is preblended with homopolymer A or B or with both.[30] However, in the present work and since the copolymer architecture is not symmetric for the two sequences, different series of experiments were performed with the additives introduced to the dispersed PS phase or to the matrix PI phase or in certain cases with the additive preblended with both homopolymers.

Images of each drop formed are digitized every 10 min for long periods of time, and the profiles are analyzed. Viscoelastic and interfacial equilibria are considered to have been attained when the extracted values of the interfacial tension do not change with time.[5−7] Caution is always taken to avoid degradation of (especially) the PI for long times at 140 °C, where all the measurements reported herein were carried out. The samples are always under an inert (nitrogen) atmosphere, and in most cases the viscosity of the PI matrix is checked after the end of the measurements.

Densities. Literature values were used for the calculation of the densities of PS and PI homopolymers. The density of PS is estimated from[42]

$$1/\rho_{PS} = 0.9199 + (5.098 \times 10^{-4})(T - 273) + (2.354 \times 10^{-7})(T - 273)^2 + \frac{32.46 + 0.1017(T - 273)}{M_{w,PS}} \quad (1)$$

where ρ_{PS} is in g/cm^3, T is in Kelvin, and $M_{w,PS}$ is the weight average molecular weight of PS. The density of PI is similarly estimated from[43]

$$1/\rho_{PI} = 1.0771 + (7.22 \times 10^{-4})(T - 273) + (2.346 \times 10^{-7})(T - 273)^2 \quad (2)$$

where ρ_{PI} is in g/cm^3. Since the weight fractions of copolymers added is always small (less or equal to 4%), it is assumed that the addition does not affect appreciably the density difference across the interface. The maximum possible uncertainty this assumption introduces is less than 2.7% for all the concentrations investigated and less than 1.4% for the 2 wt % concentration; this is well within the error bars of the measurements. It should be noted that the accuracy in the extracted values of the interfacial tension is directly proportional to the accuracy in the estimation of the density difference $\Delta\rho$.

Small-Angle X-ray Scattering. Small-angle X-ray scattering (SAXS) experiments were performed on mixtures of polyisoprene with the various polystyrene-*block*-polyisoprene copolymers utilizing a Rigaku 2263A3 camera with slit collimation (slits 0.03 mm at a distance of 112 mm apart) equipped with a one-dimensional position-sensitive detector (straight metal wire). The sample to detector distance was 280 mm, so that scattering wave vectors $q = (4\pi/\lambda)\sin(\theta/2)$ as low as 0.012 Å^{-1} could be measured without interference from the beam stop (θ is the scattering angle, and λ is the wavelength of the X-rays). The X-rays were produced by a Rigaku 12 kW rotating anode X-ray generator, and Cu Kα radiation was used ($\lambda = \lambda_{Cu\ K\alpha} = 1.54$ Å). The smeared intensities were collected in a multichannel analyzer and transferred to an HP workstation for further analysis. The data have been corrected for absorption, background scattering, and slit-length smearing. The background correction was made by subtracting from the total intensity the contribution of density fluctuations evaluated from measuring pure PS and pure PI (at the same temperature) and calculating the weighted average on the basis of the composition of the sample in PS and PI. Desmearing was performed (when explicitly stated) using an algorithm developed by Strobl.[44] In principle, analysis of the SAXS data can be performed following the method outlined by Roe and coworkers[45] for the determination of the micelle characteristics. However, the micelles were too large for the scattering vector range of our SAXS camera, and therefore, it was not possible to extract information on their size.

III. Results and Discussion

Experimental Interfacial Tension Data. Figure 1 shows the interfacial tension data γ for two PS/I_2S/PI systems as a function of copolymer concentration at a constant temperature of 140 ± 1 °C for two different situations. In the first, the I_2S-4 graft copolymer was premixed with the PS homopolymer and the mixture was used to form the drop in a PI matrix [(PS + I_2S-4)/PI]. In the second case, the I_2S-4 graft was preblended with the PI and the mixture formed the matrix where

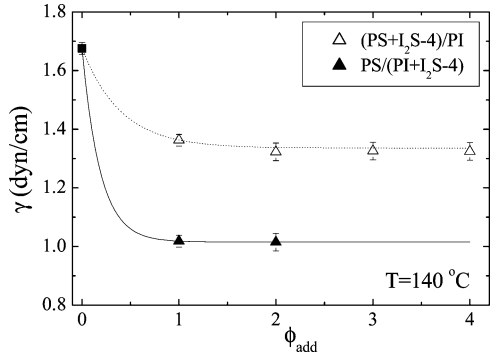

Figure 1. Interfacial tension for the PS/I_2S-4/PI systems as a function of copolymer concentration added to the polystyrene phase (open symbols) or to the polyisoprene phase (solid symbols) at a constant temperature of 140 ± 1 °C for graft copolymer I_2S-4. The lines are guides to the eye,[46] whereas the solid square (■) denotes the PS/PI interfacial tension in the absence of the copolymer.

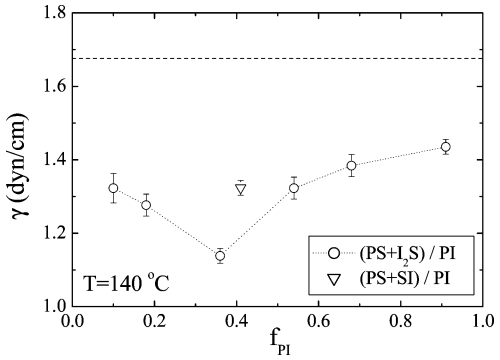

Figure 2. Interfacial tension for the (PS + I_2S)/PI systems as a function of the composition of the graft copolymers at a constant temperature of 140 ± 1 °C and constant 2 wt % copolymer added to the polystyrene phase (○). ▽ denotes the interfacial tension for (PS + SI)/PI at 140 ± 1 °C, i.e., with the addition of 2 wt % SI diblock copolymer to the polystyrene phase. The dashed line indicates the PS/PI interfacial tension in the absence of the copolymers.

PS homopolymer formed the drop [(PS/(PI + I_2S-4)]. The copolymer concentration is expressed as the weight of the copolymer per weight of the homopolymer. A sharp decrease in the interfacial tension is observed with addition of small amounts of the graft copolymer, once more illustrating the expected surfactant-like behavior of the copolymer. The interfacial tension levels off as the additive concentration increases to a value of γ_{sat}; this is usually attributed to interfacial saturation and/or to micelle formation by the copolymer. These observations are in agreement with previous investigations on other systems.[46] The differences in the two different series of measurements will be discussed in relation to Figure 3 below.

Figure 2 shows the interfacial tension data for the (PS + I_2S)/PI systems with 2 wt % graft copolymer at a constant temperature of 140 ± 1 °C as a function of the composition of the graft copolymer. It is noted that, for all systems investigated, this concentration corresponds to the plateau value of interfacial tension γ_{sat}. In the same plot the interfacial tension at saturation is also shown for (PS + SI)/PI, i.e., when a diblock copolymer (of molecular weight almost equal to that of the series of graft copolymers) is used as an additive. Two observations are in order: The first one is that the effectiveness of the graft copolymer in reducing the polymer/polymer interfacial tension depends on the copolymer

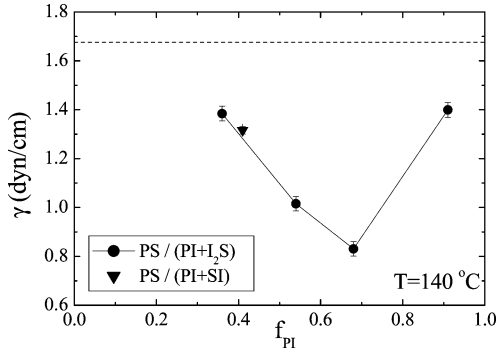

Figure 3. Interfacial tension for the PS/(PI + I_2S) systems as a function of the composition of the graft copolymers at a constant temperature of 140 ± 1 °C and constant 2 wt % copolymer added to the polyisoprene phase (●). ▼ denotes the interfacial tension for PS/(PI + SI) at 140 ± 1 °C, i.e., with the addition of 2 wt % SI diblock copolymer to the polyisoprene phase. The dashed line indicates the PS/PI interfacial tension in the absence of the copolymers.

composition. In both sides of the composition axis, the interfacial tension at saturation decreases as the short blocks become longer; i.e., the additive becomes more interfacially active when the lengths of the arms increase. It is interesting that the most effective is the graft copolymer with $f_{PI} = 0.36$. As the volume fraction of polyisoprene in the I_2S copolymer, f_{PI}, increases, the chemical potential of the copolymer in the PS phase increases because its unfavorable interactions with the PS homopolymer increase. This drives more copolymer to the polymer/polymer interface (i.e., it is expelled from the PS phase), and thus, the interfacial tension decreases even more. However, at higher volume fractions f_{PI} the interactions should lead to the formation of micelles of the copolymer within the homopolymer phase. As a result and similarly to the earlier work,[30] less and less copolymer is now driven to the interface and the interfacial tension decreases less. This explains the nonmonotonic behavior depicted in Figure 2. Note that, indeed, for large PI content, a slight cloudiness was observed in the PS + I_2S mixtures, indicating some kind of micellar aggregation. The second observation in Figure 2 concerns the fact that the best value for I_2S-3 and also the value for I_2S-2 are lower than that for the symmetric linear diblock copolymer of the same total molecular weight (all in the plateau region of the interfacial tension reduction). It appears that the old rule of thumb "diblocks better than triblocks better than grafts" should be reconsidered in the general case. The graft I_2S-3 has a composition ($f_{PI} = 0.36$) very similar to that of diblock SI ($f_{PI} = 0.41$) and very similar molecular weight, but it is more interfacially active, which most probably is an architecture effect. The better efficiency of the graft copolymer versus that of the diblock is not anticipated theoretically[22] (when micelles are not considered), but it is in agreement with an early study[47] on (polystyrene)(poly(ethylene oxide))$_2$ grafts versus polystyrene−poly(ethylene oxide) diblocks of similar molecular weights. It is believed that this is due to the higher tendency of the diblock to form micelles.

Since the PS/I_2S/PI systems are not symmetric in both the architecture and the composition, one has to investigate the behavior when the additive is preblended with the matrix homopolymer as well. Figure 3 shows the interfacial tension data for the PS/(PI + I_2S) systems with 2 wt % graft copolymer at a constant temperature of 140 ± 1 °C as a function of the composition of the

graft copolymer. Again, for these systems this concentration corresponds to the plateau value of interfacial tension γ_{sat} in each case. Right away one can observe that the data for two of the graft copolymers (I_2S-1 and I_2S-2) with low f_{PI} are missing from Figure 3. This is due to the fact that their mixtures with PI were optically not clear because of immiscibility, and thus, it was impossible to measure the profile of the PS drops within these matrices. The interfacial tension at saturation data show the behavior of Figure 2 in that the additive becomes more efficient when the length of the short arms increases. The explanation is similar to that discussed in relation to Figure 2. Since now the additive is introduced in the polyisoprene phase, as f_{PI} decreases from the highest value the interactions of the copolymer with the homopolymer become more unfavorable (the chemical potential of the copolymer in the PI phase increases), thus driving more copolymer toward the interface and reducing the interfacial tension. However, at lower values of f_{PI}, as f_{PI} decreases the copolymer forms micelles (and apparently even phase separates for I_2S-1 and I_2S-2), and thus, its interfacial activity is reduced. However, the values of the interfacial tension at saturation are significantly lower than those obtained when the additive was introduced in the PS phase, whereas the most efficient additive is I_2S-5 with $f_{PI} = 0.68$, i.e., the one with three equal arm lengths. This copolymer, however, has a very significant amount of polyisoprene, and thus, when it is preblended with the polystyrene homopolymer, it apparently forms micelles, which hinders its interfacial activity. When introduced to the polyisoprene phase, however, it does not form micelles nor does it phase separate, and thus, its interfacial activity can be expressed.

We are aware of only two earlier studies which discussed that the interfacial tension at saturation may depend on the side of the interface where the additive has been introduced.[7a,48] Right away this observation sheds doubts on the state of equilibrium of the experimental system. As noted in the Experimental Section, images of the drops formed are digitized every 10 min for long periods of time, and the profiles are analyzed; "equilibrium" is considered to have been attained when the extracted values of the interfacial tension do not change with time. Apparently, however, the two different situations do not lead to the same equilibrium but rather to two different stationary states of "local equilibrium". It is believed that these pseudoequilibrium situations correspond to the situation where the additive has segregated to the interface but has not crossed the interface toward the other homopolymer phase. To probe this, a (polystyrene)$_2$(polyisoprene) simple graft copolymer of the mirror image architecture was utilized with composition $f_{PI} = 0.53$, and the interfacial tension was measured when the additive was introduced in either the PS or the PI phase.

Figure 4 shows all the interfacial tension data discussed so far together with those for S_2I. For the I_2S grafts the behavior of Figures 2 and 3 is depicted when the graft is introduced to the PS or the PI phase. For the symmetric SI diblock the interfacial tension at saturation does not depend on whether the additive is premixed with the PS or the PI phase;[30] i.e., in that case, adding the copolymer to the drop or the matrix phase did not make any difference. Thus, the SI data allow us to rule out one of the possible explanations discussed by Hu et al.,[7a] who suggested that the effect may be due

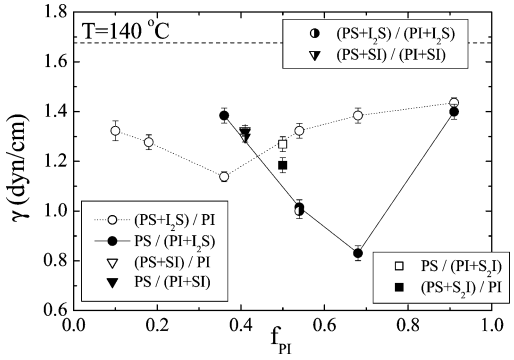

Figure 4. Interfacial tension for the PS/I_2S/PI systems as a function of the composition of the graft copolymers at a constant temperature of 140 ± 1 °C and constant 2 wt % copolymer added to the polystyrene (○) or the polyisoprene (●) phase or when 1 wt % was added to the polystyrene phase and 1 wt % to the polyisoprene phase (black and white circle). Also shown are the interfacial tension data for PS/SI/PI at 140 ± 1 °C, i.e., with the addition of 2 wt % SI diblock copolymer to the polystyrene (▽) or the polyisoprene (▼) phase or when 1 wt % was added to the polystyrene phase and 1 wt % to the polyisoprene phase (black and white inverse triangle). The squares are the interfacial tension data for PS/S_2I/PI at 140 ± 1 °C when 2 wt % S_2I was added to the polystyrene (■) or the polyisoprene (□) phase. The dashed line indicates the PS/PI interfacial tension in the absence of the copolymers.

to the presence of a larger reservoir of diblock when added in the matrix phase versus a depletion when added to the drop phase. The interfacial tension at saturation data for the S_2I graft copolymer follow the mirror image of the dependencies shown before for the I_2S: The data for (PS + S_2I)/PI follow the behavior of PS/(I_2S + PI), and the data for PS/(S_2I + PI) follow that of (PS + I_2S)/PI. This clearly signifies that it is indeed the attainment of local equilibrium with the additive not crossing to the other side of the interface that is responsible for the behavior of Figures 2−4. Such an explanation was also discussed in ref 7a for the PS-*block*-poly(dimethylsiloxane), PS-*b*-PDMS, case. It is believed that in the present case it is the asymmetric architecture of the graft copolymers that leads to this great disparity between the two cases, whereas it should probably be the asymmetry in the statistical segment lengths of the two blocks in the PS-*b*-PDMS case that leads to an asymmetry in the critical micelle concentration and, thus, in the interfacial tension reduction. One last point with respect to Figure 4 relates to the interfacial tension data when 1 wt % I_2S-4 was introduced to PS and 1 wt % to PI: in this case the interfacial tension reduction is that of the lower of the two cases; i.e., that for (PS + I_2S-4)/(PI + I_2S-4) is the same with that for PS/(PI + I_2S-4).[49]

The overall message of Figure 4 is that the copolymer with the highest interfacial activity is a graft copolymer with three equal arm lengths, which, however, should be added to the "correct" side of the interface, i.e., to the homopolymer that is identical to that of the backbone of the graft copolymer. The correct side of the interface is most probably determined by the need to avoid the possibility of micellar formation by the copolymer; this will also be discussed in the Theoretical Considerations. The differentiation between the two sides of the interface is believed to be due to the trapping of the copolymers when they reach the interface; if the additives were able to cross the interface, then there would not be any differentiation of the two sides of the interface.

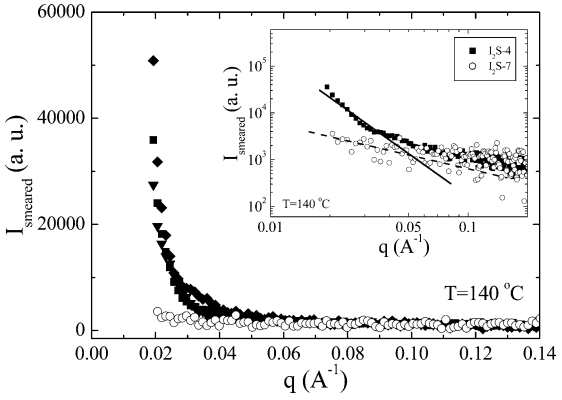

Figure 5. Smeared small-angle X-ray scattering intensity (in arbitrary units) for 2 wt % blends of the various graft copolymers with the polyisoprene homopolymer at 140 °C as a function of the scattering vector q: (◆) I_2S-3, (■) I_2S-4, (▼) I_2S-5, and (○) I_2S-7. The inset shows the double logarithmic representation of the scattering intensity versus q for (■) I_2S-4 and (○) I_2S-7, with the two lines indicating slopes −3 (solid line) and −1 (dotted line), respectively.

SAXS Measurements. To verify that the absence or the formation of micelles is the reason for the nonmonotonic dependence of γ_{sat} on the graft copolymer composition, small-angle X-ray scattering measurements were performed on homopolymer/copolymer mixtures as a function of concentration, copolymer composition, and temperature. Figure 5 shows the (smeared) scattering intensity for 2 wt % blends of the various grafts with the PI homopolymer at the temperature of the interfacial tension measurements (140 °C) as a function of the scattering vector q. It is noted that the scattering from homopolymer PI at the same conditions and at the same temperature has been subtracted from the data of the blends to subtract the contribution of density fluctuations. Thus, the scattering in Figure 5 corresponds only to concentration fluctuations. It is evident that the scattering intensity is very low for the graft copolymer with the highest amount of polyisoprene whereas it significantly increases (with a pronounced q dependence) for the grafts with lower polyisoprene content. This signifies the absence of micelles in the blend with the highest $f_{PI} = 0.91$ (I_2S-7) and the presence of micelles in the blends with lower f_{PI} values.

The inset of Figure 5 demonstrates the wave vector dependence of the smeared scattering intensity in a double logarithmic representation for blends with copolymers I_2S-7 ($f_{PI} = 0.91$) and I_2S-4 ($f_{PI} = 0.54$), which correspond to the two sides of the minimum in Figure 3. The intensity data for the blend with I_2S-7 exhibit an $I_{smeared} \propto q^{-1}$ dependence, whereas those for the blend with I_2S-4 decrease with q as $I_{smeared} \propto q^{-3}$. The q^{-3} dependence for the smeared intensity corresponds to the case of scattering from a two-phase system with sharp interfaces in the Porod[50] limit for slit collimation: for large q, $I \propto q^{-4}$ for pinhole collimation and $I_{smeared} \propto q^{-3}$ for slit collimation and infinite slit width.[51,52] The q^{-1} dependence observed for I_2S-7 corresponds to the anticipated behavior for slit-smeared intensities for the Kratky region for homogeneously dispersed Gaussian chains (q^{-2} dependence for pinhole collimation and q^{-1} dependence for slit-smeared data). Therefore, this is additional strong evidence for the presence of micelles for I_2S-4 and their absence for I_2S-7. Small-angle neutron scattering studies are currently under way for the investigation of the micellar formation in the same graft copolymer/homopolymer systems to probe the dependence of the micellization in homopolymer matrices on copolymer architecture as an extension from a previous study in selective solvents.[37]

It should be noted once more[30] that the present SAXS measurements were performed on homopolymer/copolymer (PI/I_2S) mixtures whereas the interfacial tension data are for a homopolymer/copolymer/homopolymer three-component system. Therefore, the possibility for micelle formation should have been, in principle, investigated for the three-component blend. However, the small-angle scattering in that case would be dominated by the macrophase-separated morphology, whereas the contribution to the intensity due to the presence of micelles in either macrophase would be minimal; small-angle neutron scattering experiments on suitable systems with contrast variation are planned to probe the actual situation. As was discussed in an earlier paper,[30] the present SAXS data are in principle directly comparable with polymer/air surface tension data of PI/I_2S mixtures. There it was found that the existence of micelles influences the dependence of the surface tension on the MW in a way similar to that of the interfacial tension. Moreover, it was found that the characteristic MW for which the change in the behavior of the surface tension was observed agreed with that for which the change in the existence/absence of micelles occurred whereas the characteristic MW was somehow different than the one for the interfacial tension reduction. This was attributed to the possible different contributions to the free energy associated with a copolymer chain at the PS/PI interface versus that at a PS/air surface.[30] It is believed that the same reasoning can explain why the micelles are apparently formed for concentrations between those of I_2S-7 and I_2S-5 (from Figure 5) whereas the minimum in interfacial tension occurs for I_2S-5.

Theoretical Considerations. The emulsifying behavior of block copolymers at the polymer/polymer interface has attracted the interest of theoreticians over the last 20 years.[13−23] Noolandi and Hong[13] utilized their theory of inhomogeneous systems to investigate the segment density profiles at the interface for the system homopolymer A/homopolymer B/diblock copolymer A−B/common solvent. They investigated the effect of the molecular weight and the concentration of the diblock on the interfacial tension under the assumption that the copolymer is either localized at the interface or randomly distributed in the bulk homopolymer phases, i.e., for concentrations below the critical micelle concentration (cmc). Shull and Kramer[17] developed and applied the Noolandi−Hong theory for the case without solvent, whereas they also discussed the possibility of micelle formation in view of their earlier experimental observations.[3,28] Semenov[29] developed an analytical mean-field theory for the equilibrium of block copolymers in a homopolymer layer between an interface with another homopolymer and the free surface, which was compared to the data of Shull et al.,[3] whereas he also analyzed the situation for concentrations higher than the cmc and found that the micelles are attracted to both the free surface and (somewhat weaker) to the polymer/polymer interface, but he did not investigate the interfacial tension reduction due to the copolymer segregation to the polymer/polymer interface.

In our recent paper,[30] an attempt was made to provide a semiquantitative analysis of the interfacial activity of diblock copolymers at the polymer/polymer interface and its nonmonotonic dependence on the diblock mo-

lecular weight (at constant copolymer concentration). The attempt was based on a modification of the analysis of Leibler,[16] where the possibility of micellar formation was also taken into account. The thermodynamic equilibrium was, thus, considered among copolymer chains adsorbed at the interface, chains homogeneously distributed in the bulk homopolymers, and chains at micelles formed within the homopolymer phases. At low molecular weights, micelles do not exist and the equilibrium is achieved between copolymer chains at the interface and chains homogeneously distributed in the bulk; increasing the molecular weight drives more copolymer chains to the interface, thus decreasing the interfacial tension. At higher molecular weights, when micelles are also present, a further increase of the molecular weight drives fewer copolymer chains to the interface; thus, the interfacial tension reduction is smaller. Although the assumptions involved did not allow a quantitative comparison and no fitting was attempted, the behavior of the interfacial tension reduction as a function of the copolymer molecular weight (at constant additive concentration) resembled the experimental data.

The effects of copolymer architecture of the interfacial efficiency of the compatibilizers have been investigated in a series of papers by Balazs and co-workers[21,22] using a combination of self-consistent mean-field (SCF) calculations, analytical theory, and Monte Carlo simulations as well as by Dadmun[23] using computer simulations. Lyatskaya et al.[22] investigated the interfacial tension reduction due to the localization of AB block copolymers at the interface between two immiscible homopolymers A and B as a function of the copolymer architecture. For the same total copolymer molecular weight, for symmetric copolymers ($f = 0.5$) and for very high molecular weight homopolymers, both analytical arguments and SCF theory agree in that diblock copolymers are the most efficient at reducing the interfacial tension followed by the simple grafts, the four-armed stars, and the *n*-teeth combs. They also discussed the tradeoff between total molecular weight and number of teeth when combs and diblocks of different molecular weights are compared; i.e., they found that long combs are more efficient that short diblocks.

The analytical arguments[22] were based on the formalism that Leibler developed[16] for diblock copolymers, which was extended for the case of comb and star copolymers. Of interest in the present work is the case of simple graft copolymers, which were denoted as T-grafts and were considered as combs with $n = 1$ tooth. The homopolymers were considered to be highly incompatible, whereas the copolymer chains were assumed to form dry brushes at the interface and to be at equilibrium with chains homogeneously distributed in the bulk. For this case, the interfacial tension reduction $\Delta\gamma$ for a graft copolymer AB_2 was predicted as

$$\frac{\Delta\gamma b^2}{k_B T} = \frac{(\gamma_0 - \gamma)b^2}{k_B T} = \left(\frac{2}{\pi}\right)\left(\frac{2}{3}\right)^{3/2} N^{-1/2} {\mu_{bulk}}^{3/2} (4 - 3f_A)^{-1/2} \quad (3)$$

where γ_0 is the A/B interfacial tension in the absence of the additive, χ is the Flory−Huggins interaction parameter, N is the number of segments of the graft copolymer, $f = f_{tooth} = f_A$ is the volume fraction of the tooth block A, b is the statistical segment length (it is assumed that both types of links have the same segmental volume $v = b^3$), and $k_B T$ is the thermal energy. μ_{bulk} is the chemical potential in the bulk, and $\mu_{bulk} \approx \ln \phi_+ + \chi N f_A$ if the copolymer is added to the B homopolymer phase, where ϕ_+ is the copolymer volume fraction in the bulk B homopolymer phase (which is very close to the nominal amount of copolymer present, ϕ_{add}). Note that, within the same assumptions, the respective interfacial tension reduction for a diblock copolymer is

$$\frac{\Delta\gamma_{diblock} b^2}{k_B T} = \frac{(\gamma_0 - \gamma)_{diblock} b^2}{k_B T} = \left(\frac{2}{\pi}\right)\left(\frac{2}{3}\right)^{3/2} N^{-1/2} {\mu_{bulk}}^{3/2} \quad (4)$$

Below an attempt is made to extend these arguments for finite homopolymer molecular weights and allowing for mixing of the copolymer and homopolymer chains (wet brush or mushroom regimes) and by explicitly including in the considerations the possibility of micelle formation similarly to the earlier attempt for diblock copolymers.[30]

A flat interface is considered with surface area A_I between phase-separated A and B homopolymers. The thickness of the interfacial region $a_I = b(6\chi)^{-0.5}$ and the interfacial tension $\gamma_0 = k_B T b^{-2}(\chi/6)^{0.5}$ are independent of the number of segments P_A and P_B of the two homopolymers[53] for a highly incompatible situation of $\chi P_i \gg 1$. Suppose that Q AB_2 copolymer chains with $N = N_A + 2(N_B/2)$ segments and composition $f = f_{tooth} = N_A/N = f_A$ are adsorbed at the A/B interface (for most practical situations, $\chi N_i \gg 1$). It is expected that the copolymer joints are localized in a thin interfacial layer of thickness[29] $d' = (\pi/2)a_I$, with the blocks A and B extending toward the respective bulk layers and forming two "adsorbed layers" of thickness L_A and L_B, respectively. For $d' \ll L_i$, each side of the interfacial film resembles a layer of polymers anchored by one end onto a wall. Note that the A layer is formed by Q chains of length N_A whereas the B layer by $2Q$ chains of length $N_B/2$ each. The free energy of the interfacial film can, thus, be approximated as[16]

$$F_{interf\ film} = \gamma_0 A_I + Q(g_A + g_B) \quad (5)$$

γ_0 is the A/B interfacial tension in the absence of the additive, A is the interfacial area, and g_A and g_B represent the free energies per AB_2 chain of the A and B layers. $\sigma = Q/A_I$ is the number of copolymer chains per unit interfacial area.

In most of the present work, the copolymer chains are not so long relative to the homopolymers. Thus, mixing of the N copolymer and P homopolymer chains should be taken into account due to the homopolymers penetrating the chains anchored at the interface, whereas the copolymer chains can be either stretched (wet brush regime) or nonstretched (wet mushroom). Neglecting the composition gradients in the brush (Flory approximation), g_A is given by[2b,16,54]

$$\frac{g_A}{k_B T} = \ln(N_A b^2 \sigma) + L_A \frac{1}{\sigma b^3} \frac{1}{P_A}(1 - \eta_A)\ln(1 - \eta_A) + \frac{3}{2}\frac{{L_A}^2}{N_A b^2} \quad (6a)$$

where $\eta_A = \sigma N_A b^3 / L_A$ is the average volume fraction of monomers of the A block in the layer and $1 - \eta_A$ is that of the P_A monomers. The first two terms approximate the entropy of mixing between N and P chains, which

tend to swell the copolymer blocks; the first term is associated with the translational freedom of the copolymers in the two-dimensional film, whereas the second one originates from the translational entropy of the P chains and has a standard excluded volume form.[54] The last term represents the elastic entropy term, which limits the swelling. For low values of $\eta_A \ll 1$, eq 6a can be written as[2b,16]

$$\frac{g_A}{k_B T} = \ln(N_A b^2 \sigma) + \frac{1}{2}\frac{N_A \eta_A}{P_A} + \frac{3}{2}\frac{{L_A}^2}{N_A b^2} \qquad (7a)$$

For stretched chains, the brush thickness L_A and the block monomer concentration η_A are obtained from eq 7a by minimization with respect to L_A. In this case, $L_A = 6^{-1/3} N_A b (\sigma b^2)^{1/3} {P_A}^{-1/3}$, $\eta_A = 6^{1/3}(\sigma b^2)^{2/3} {P_A}^{1/3}$, and

$$\frac{g_A}{k_B T} = \ln(N_A b^2 \sigma) + \frac{3^{4/3}}{2^{5/3}}(\sigma b^2)^{2/3} N_A {P_A}^{-2/3} \text{ (wet brush)} \qquad (8a)$$

which is valid for $P_A N_A^{-3/2} < \sigma b^2 < {P_A}^{-1/2}$. For nonstretched chains, $L_A \approx {N_A}^{1/2} b$ and the last term of eq 7a can be neglected; this applies for[54] $\sigma b^2 < P_A N_A^{-3/2}$. Then, $\eta_A = \sigma b^2 {N_A}^{1/2}$ and

$$\frac{g_A}{k_B T} = \ln(N_A b^2 \sigma) + \frac{1}{2}\frac{{N_A}^{3/2}\sigma b^2}{P_A} \text{ (wet mushroom)} \qquad (8b)$$

For diblock copolymer chains at the interface, the analysis for the B layer is the same as that for the A layer with simply replacing A with B as the subscript in the equations above. However, for an AB_2 simple graft, the equations for the free energy should reflect the fact that the B layer is formed by two B blocks per AB_2 chain. Thus, g_B is given by

$$\frac{g_B}{k_B T} = \ln(N_B b^2 \sigma) + L_B \frac{1}{\sigma b^3}\frac{1}{P_B}(1-\eta_B)\ln(1-\eta_B) + 2\frac{3}{2}\frac{{L_B}^2}{(N_B/2)b^2} \qquad (6b)$$

with $\eta_B = \sigma N_B b^3 / L_B$, the average volume fraction of monomers of B chains. For low values of $\eta_B \ll 1$, eq 6b can be written as[2b,16]

$$\frac{g_B}{k_B T} = \ln(N_B b^2 \sigma) + \frac{1}{2}\frac{(N_B/2)\eta_B}{P_B} + 2\frac{3}{2}\frac{{L_B}^2}{(N_B/2)b^2} \qquad (7b)$$

As before, for stretched chains L_B and η_B are obtained from eq 7b by minimization with respect to L_B; thus, $L_B = (1/2)6^{-1/3} N_B b (\sigma b^2)^{1/3} {P_B}^{-1/3}$, $\eta_B = (2)6^{1/3}(\sigma b^2)^{2/3} {P_B}^{1/3}$, and

$$\frac{g_B}{k_B T} = \ln(N_B b^2 \sigma) + \frac{3^{4/3}}{2^{5/3}}(\sigma b^2)^{2/3} N_B {P_B}^{-2/3} \text{ (wet brush)} \qquad (8c)$$

which is valid for $P_B(N_B/2)^{-3/2} < \sigma b^2 < {P_B}^{-1/2}$. For nonstretched chains, $L_B \approx (N_B/2)^{1/2} b$ and the last term of eq 7b can be neglected; this applies for[54] $\sigma b^2 < P_B (N_B/2)^{-3/2}$. Then, $\eta_B = \sigma b^2 (2N_B)^{1/2}$ and

$$\frac{g_B}{k_B T} = \ln(N_B b^2 \sigma) + \frac{1}{2^{3/2}}\frac{{N_B}^{3/2}\sigma b^2}{P_B} \text{ (wet mushroom)} \qquad (8d)$$

The interfacial tension in the presence of the copolymer is calculated as[55]

$$\gamma = \left.\frac{\partial F_{\text{interf film}}}{\partial A}\right|_Q = \gamma_0 - \sigma^2\left(\frac{\partial g_A}{\partial \sigma} + \frac{\partial g_B}{\partial \sigma}\right) \qquad (9)$$

with g_A and g_B given by eqs 8a−d. Therefore, the interfacial tension reduction, $\Delta\gamma = \gamma_0 - \gamma$, is

$$\frac{\Delta\gamma}{k_B T} = \frac{\gamma_0 - \gamma}{k_B T} = \begin{cases} \sigma\left[2 + \frac{3^{1/3}}{2^{2/3}}(\sigma b^2)^{2/3}(N_A {P_A}^{-2/3} + N_B {P_B}^{-2/3})\right] & \text{(wet brush)} \\ \sigma\left[2 + \frac{1}{2}\sigma b^2 ({N_A}^{3/2} {P_A}^{-1} + 2^{-1/2} {N_B}^{3/2} {P_B}^{-1})\right] & \text{(wet mushroom)} \end{cases} \qquad (10)$$

At equilibrium, σ is determined by equating the chemical potential of the copolymer chains at the interface with that of the copolymer chains either homogeneously mixed with the homopolymers or at micelles formed within the homopolymer phases. The chemical potential of a copolymer chain at the interface is calculated using eq 5 as

$$\mu_{\text{int}} = \left.\frac{\partial F_{\text{interf film}}}{\partial Q}\right|_A = g_A + g_B + \sigma\left(\frac{\partial g_A}{\partial \sigma} + \frac{\partial g_B}{\partial \sigma}\right) \qquad (11)$$

Therefore, with eqs 8

$$\frac{\mu_{\text{int}}}{k_B T} = 2 + \ln(N_A \sigma b^2) + \ln(N_B \sigma b^2) + \begin{cases} 2.271(\sigma b^2)^{2/3}(N_A {P_A}^{-2/3} + N_B {P_B}^{-2/3}) & \text{(wet brush)} \\ \sigma b^2 ({N_A}^{3/2} {P_A}^{-1} + 2^{-1/2} {N_B}^{3/2} {P_B}^{-1}) & \text{(wet mushroom)} \end{cases} \qquad (12)$$

The free energy density of a homogeneous mixture of an A−B copolymer (irrespective of architecture) with an A homopolymer is[29]

$$\frac{F_{\text{bulk}}}{k_B T} = \frac{\phi}{N}\ln\left(\frac{\phi}{e}\right) + \frac{1-\phi}{P_A}\ln\left(\frac{1-\phi}{e}\right) + \chi\phi f_B(1 - f_B\phi) \qquad (13)$$

with $f_B = 1 - f_A$. Thus, the chemical potential of a copolymer chain homogeneously distributed in the bulk A homopolymer, $\mu_{\text{bulk}} = N[(1-\phi)(\partial F_{\text{bulk}}/\partial\phi) + F_{\text{bulk}}]$, is

$$\frac{\mu_{\text{bulk}}}{k_B T} = \ln\phi - \phi - (1-\phi)\frac{N}{P_A} + \chi N f_B[1 - 2f_B\phi + f_B\phi^2] \qquad (14a)$$

where $\phi = \phi_-$ is the copolymer volume fraction in the A-rich homopolymer phase. When the graft copolymer is added to the B homopolymer phase, the bulk chemical potential is

$$\frac{\mu_{\text{bulk}}}{k_B T} = \ln\phi - \phi - (1-\phi)\frac{N}{P_B} + \chi N f_A[1 - 2f_A\phi + f_A\phi^2] \qquad (14b)$$

For the calculation of the chemical potential of the copolymer chains in a micelle, we use the methodology that Leibler[16] demonstrated for the case of diblock copolymers as was also done by Lyatskaya et al.[22] However, for the case of AB_2 graft copolymers one has to distinguish two different cases: one when the micelle is formed within the A homopolymer phase, i.e., when the two B blocks form the core and the A block forms the corona of the micelle, and one when the micelle is formed within the B homopolymer, i.e., when the "tooth" A block forms the core of the micelle and the two B blocks form the corona. The two cases are considered in the Appendix for the three different cases of formation of spherical, cylindrical, or lamellar micelles. The chemical potential of an AB_2 chain in a micelle formed within the A phase is, thus

$$\frac{\mu_{\text{mic}}^{\text{spherical}}}{k_{\text{B}}T} = (3/2)^{4/3}(1-f_{\text{A}})^{4/9}[3.96(1-f_{\text{A}})^{-1/3}-1]^{1/3}(\chi N)^{1/3}$$

$$\frac{\mu_{\text{mic}}^{\text{cylindrical}}}{k_{\text{B}}T} = 1.19(\chi f_{\text{A}} N)^{1/3}[6.57-\ln(1-f_{\text{A}})]^{1/3} \quad (15a)$$

$$\frac{\mu_{\text{mic}}^{\text{lamellar}}}{k_{\text{B}}T} = 1.57(\chi N)^{1/3}(1.44-f_{\text{A}})^{1/3}$$

whereas the chemical potential of an AB_2 chain in a micelle formed within the B phase is

$$\frac{\mu_{\text{mic}}^{\text{spherical}}}{k_{\text{B}}T} = (3/2)^{4/3} f_{\text{A}}^{4/9}(4.74 f_{\text{A}}^{-1/3}-4)^{1/3}(\chi N)^{1/3}$$

$$\frac{\mu_{\text{mic}}^{\text{cylindrical}}}{k_{\text{B}}T} = 1.89(\chi f_{\text{A}} N)^{1/3}(0.41-\ln f_{\text{A}})^{1/3} \quad (15b)$$

$$\frac{\mu_{\text{mic}}^{\text{lamellar}}}{k_{\text{B}}T} = 1.75(\chi N)^{1/3}(1.26-f_{\text{A}})^{1/3}$$

For the cases when micelles are not present, the equilibrium is established between copolymer chains homogeneously distributed within the homopolymer phase and copolymer at the interface. The surface density σ is, then, determined by

$$\mu_{\text{int}}(\sigma) = \mu_{\text{bulk}}(\phi_{\pm}) \quad (16)$$

where, in this case, it is assumed that $\phi = \phi_{\pm} \cong \phi_{\text{add}}$. When micelles are present, then at thermodynamic equilibrium σ is determined by the equation

$$\mu_{\text{int}}(\sigma) = \mu_{\text{mic}} = \mu_{\text{bulk}}(\phi_{\pm}) \quad (17)$$

which also determines the volume fraction $\phi_{\pm}$ of copolymers remaining homogeneously distributed in the bulk A or B phase.

For the calculation of the interfacial tension reduction, the chemical potentials μ_{int}, μ_{mic}, and μ_{bulk} are evaluated as a function of σ for $\phi = \phi_{\pm} = \phi_{\text{add}}$. If $\mu_{\text{bulk}}(\phi_{\text{add}}) < \mu_{\text{mic}}$, the equilibrium exists between copolymers at the interface and copolymers homogeneously mixed in the homopolymer phase. The interfacial excess σ is, then, determined by eq 16 together with eqs 12 and 14, and the interfacial tension reduction $\Delta\gamma$ by eq 10. If $\mu_{\text{bulk}}(\phi_{\text{add}})$ $> \mu_{\text{mic}}$, equilibrium is established among the three different states of the copolymer (the equilibrium shape of the micelle is that corresponding to the lower $\mu_{\text{mic}}$of the three in eq 15a or 15b), whereas σ and $\phi_{\pm}$ are determined by eq 17 together with eqs 12, 14, and 15; $\Delta\gamma$ is evaluated by eq 10. Note that, due to the asymmetric architecture and in view of the experimental data presented in the previous section, two situations are considered: one when the AB_2 diblock is added to the A homopolymer (I_2S added to the polystyrene phase) and one when it is added to the B homopolymer (I_2S added to polyisoprene).

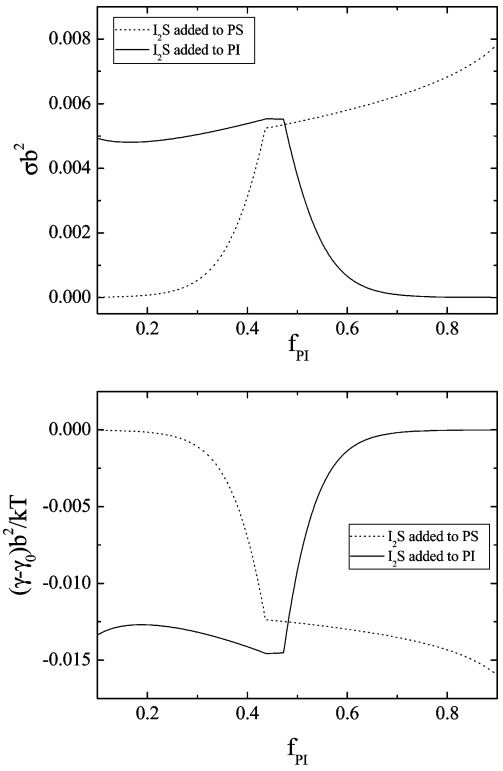

Figure 6. Theoretically estimated surface density of copolymer chains adsorbed at the interface, σb^2 (a, top), and interfacial tension reduction, $-\Delta\gamma b^2/kT = (\gamma - \gamma_0)b^2/kT$ (b, bottom), for the PS/I_2S/PI systems according to the model presented in the text as a function of the copolymer composition at constant 2 wt % copolymer concentration and for constant $\chi = 0.04$. In both (a) and (b), dotted lines signify addition of the graft copolymer to the polystyrene phase and solid lines its addition to the polyisoprene phase.

Although the assumptions involved do not allow a quantitative comparison with the data, the behavior of the estimated $\Delta\gamma$ when the graft copolymers of varying compositions are introduced into the polyisoprene or polystyrene homopolymer (at constant additive concentration) resembles more or less the experimental data. Figure 6a shows the estimated surface density of copolymers at the A/B interface, σb^2, whereas Figure 6b shows the interfacial tension reduction as $-\Delta\gamma b^2/kT = (\gamma - \gamma_0)b^2/kT$ as a function of f_{PI} for $\phi_{\text{add}} = 0.02$. The parameters used are $P_{\text{A}} = P_{\text{PS}} = 112$, $P_{\text{B}} = P_{\text{PI}} = 81$, $\chi = 0.04$, and $N = 1100$ for all grafts. Moreover, for the present range of P_i and N_i values, the wet mushroom configuration for the adsorbed copolymer chains is assumed. When the I_2S graft copolymer is added to the PI homopolymer, there are no micelles formed for high values of f_{PI} and the copolymer chains at the interface are at equilibrium with chains homogeneously mixed within the PI phase. The surface density of chains

increases with decreasing f_{PI} (from its high value), and the interfacial tension decreases. At lower values of f_{PI}, micelles are also present and σ does not increase (and even decreases) as f_{PI} decreases further; as a result the interfacial tension does not decrease further (and even increases). Similarly, when the I_2S copolymer is added to the PS homopolymer, there are no micelles formed for low values of f_{PI} and the copolymer chains at the interface are at equilibrium with chains homogeneously mixed with PS. The surface density of chains increases with increasing f_{PI}, and the interfacial tension decreases. At higher values of f_{PI}, micelles are also present and σ seizes to increase as f_{PI} increases further; as a result the interfacial tension does not decrease further. The $\Delta\gamma$ values are more or less in the range of the experimental values although the apparent functional form of the curves is different from the experimental ones. For example, the dependencies in the region where micelles are present are apparently different from the experimental ones. This is most probably due to the assumptions involved in the estimation of the chemical potentials for the copolymer chains in micelles (dry brush behavior was assumed). Even more, the value of the interaction parameter used affects both the location of the minimum (with respect to f_{PI}) and the values of $\Delta\gamma$; no fitting was attempted since the aim of the theoretical analysis is to obtain only the trends to understand the behavior of the experimental data. Indeed, it is evident that the calculation indicates a behavior very similar to the data, with the origin of this trend evidently related to the behavior of the estimated interfacial density of adsorbed chains, σ, shown in Figure 6a.

IV. Concluding Remarks

The emulsifying effect of simple graft copolymer additives on the interfacial tension between two immiscible homopolymers has been investigated using the pendant drop technique. The effects of macromolecular architecture, copolymer composition, and concentration of the additives were studied utilizing polystyrene/polyisoprene blends in the presence of a series of I_2S and a S_2I graft copolymers. The graft copolymers possess almost constant molecular weight and varying composition. As expected, the interfacial tension decreases with the addition of small amounts of copolymer followed by a leveling off as the copolymer concentration increases, illustrating the surfactant-like behavior of the graft copolymers. The interfacial tension at interfacial saturation is a nonmonotonic function of the copolymer composition f_{PI}, which can be understood to be due to the competition between the decreased affinity of the copolymer within the homopolymer phase when the size of the "incompatible" block increases, which increases the driving force of the copolymer toward the interface, and the possibility of micelle formation. These ideas are supported by small-angle X-ray scattering measurements, which show the formation or absence of micelles. Moreover, the interfacial tension at saturation depends on the side of the interface the copolymer is added; adding the I_2S graft copolymer to the polyisoprene phase is much more efficient than adding it to polystyrene. This points to a local equilibrium that is only attained in such systems: the copolymer reaching the interface from one homopolymer phase does not diffuse to the other phase. Using the respective S_2I graft, a mirror image behavior was obtained, signifying that this behavior is not a kinetic effect but is rather due to the attainment of a stationary state of local equilibrium and a lack of global equilibrium in these interfacial systems. A theoretical model proposed shows the same qualitative behavior, but it cannot quantitatively account for the effects due to assumptions involved in the estimation of the free energies of the various chain conformations and especially those within the micelles of various morphologies (certain of these have been first considered in the context of the present work).

It is therefore evident that the effectiveness of the interfacial modifiers is controlled by the unfavorable interactions, which drive the additive toward the interface, and the formation of micelles, which reduce the emulsifying activity. For nonsymmetric copolymer architectures, the latter is affected by the side of the interface where the additive is introduced, and thus, in most practical situations this should be taken seriously into consideration.

Acknowledgment. We thank K. Hong for kindly providing the polyisoprene homopolymer used in the present study as well as the diblock copolymer SI (also used in ref 30 and identified as D-5). We acknowledge that part of this research was sponsored by NATO's Scientific Affairs Division in the framework of the Science for Peace and Science for Stability Programmes and by the Greek General Secretariat of Research and Technology.

Appendix

The chemical potential of a copolymer chain within a micelle is calculated following the methodology that Leibler[16] presented for the case of diblock copolymers and for long homopolymer chains, which do not penetrate the corona of the micelles. Leibler[16] considered spherical diblock copolymer micelles, whereas the same procedure was extended by Shull et al.[3] for cylindrical and lamellar diblock copolymer micelles and by Lyatskaya et al.[22] for spherical micelles of simple AB_2 grafts. Here we present the complete calculation for both diblock AB and graft AB_2 copolymers (added in either A or B homopolymers) and for all three geometries (spherical, cylindrical, lamellar).

A.1. A−B Diblock Copolymer within a B Homopolymer. Spherical Micelles. Leibler[16] considered monodisperse spherical micelles formed by Q_m diblock copolymer A−B chains added to a B homopolymer. In this case, the A blocks make a core of radius

$$R_A = \left(\frac{3}{4\pi}\right)^{1/3}(Q_m f_A N b^3)^{1/3} \qquad \text{(A.1)}$$

whereas the B blocks form the corona, which extends up to radius R. The free energy of the micelle is represented by a sum of three contributions:

$$F_{mic} = A\gamma_0 + F_{core} + F_{corona} \qquad \text{(A.2)}$$

where $A = 4\pi R_A^2$ is the interfacial area and γ_0 is the A/B interfacial tension. The core free energy is associated with the nonuniform stretching of the A block arising from constraining the copolymer A−B junction to a narrow interface. This energy has been calculated self-consistently by Semenov[57] as[16]

$$F_{core}/kT = \left(\frac{3}{4}\right)^{5/3}\left(\frac{\pi^{4/3}}{20}\right)Q_m{}^{5/3}(f_A N)^{-1/3} \qquad \text{(A.3)}$$

Equation A.3 is identical to $F_{core}/kT = 0.370Q_mR_A^2/(f_ANb^2)$, with the constant 0.37 calculated by Semenov.[57] The free energy of the corona is calculated assuming that all the free ends of the B blocks reach the radius R and that there is no penetration of the homopolymer chains into the corona but taking into account the nonuniform deformation of the B blocks due to the spherical geometry. Thus[16]

$$F_{corona}/kT = \frac{3}{2b^2}Q_m\int_{R_A}^{R} dr\,\frac{dr(n)}{dn} \qquad (A.4)$$

where $dr(n)/dn = Q_mb^3/(4\pi r^2)$ represents the stretching of the classical trajectory $r(n)$ for the segment number n. Assuming incompressibility, the radius R is

$$R = \left(\frac{3}{4\pi}\right)^{1/3}(Q_mNb^3)^{1/3} \qquad (A.5)$$

Therefore

$$F_{corona}/kT = \frac{1}{2}\left(\frac{3}{4\pi}\right)^{2/3}Q_m^{5/3}N^{-1/3}(f_A^{-1/3} - 1) \qquad (A.6)$$

The equilibrium value of Q_m is obtained by minimizing F_{mic}/Q_{mic} with respect to Q_m, $\partial(F_{mic}/Q_m)/\partial Q_m = 0$, whereas the chemical potential is determined by

$$\mu_{mic} = F_{mic}/Q_m|_{Q=Q_{m_{min}}} \qquad (A.7)$$

where $Q_{m_{min}}$ is the value at the minimum of F_{mic}/Q_m. Thus, $Q_{m_{min}} = (3/2)^{1/2}(4\pi/3)\chi^{1/2}Nf_A^{2/3}(1.74f_A^{-1/3} - 1)^{-1}$, whereas the chemical potential for a A−B diblock copolymer chain in a micelle within homopolymer B is

$$\frac{\mu_{mic}^{spherical}}{k_BT} = (3/2)^{4/3}f_A^{4/9}(1.74f_A^{-1/3} - 1)^{1/3}(\chi N)^{1/3} \qquad (A.8)$$

which is eq A-8 of Shull et al.[3] and is consistent with eq 21 of Lyatskaya et al.[22] and eq 36 of Semenov.[29]

Cylindrical Micelles. Shull et al.[3] presented the analysis for the case of cylindrical micelles. In this case, the A blocks make a core of radius

$$R_A = (Q_mf_ANb^3/(\pi L))^{1/2} \qquad (A.9)$$

where L is the length of the cylindrical micelle. The B blocks form the corona, which extends up to radius R:

$$R = (Q_mNb^3/(\pi L))^{1/2} \qquad (A.10)$$

The free energy of the micelle is represented by a sum of three contributions:

$$F_{mic} = A\gamma_0 + F_{core} + F_{corona} \qquad (A.11)$$

where $A = 2\pi R_AL$ is the interfacial area and γ_0 the A/B interfacial tension. The core free energy is given by

$$F_{core}/kT = \frac{0.616Q_mR_A^2}{f_ANb^2} \qquad (A.12)$$

(the factor 0.616 was calculated by Semenov[57]), whereas that of the corona is given by eq A.4, with the stretching of the classical trajectory given by $dr(n)/dn = Q_mb^3/(2\pi Lr)$. Therefore

$$F_{corona}/kT = -\frac{3}{8\pi}Q_m^2bL^{-1}\ln f_A \qquad (A.13)$$

The equilibrium value of Q_m is obtained by minimizing F_{mic}/Q_m with respect to Q_m as $Q_{m_{min}} = 3.3246(\chi f_AN)^{1/3}(L/b)(1.64 - \ln f_A)^{-2/3}$, whereas the chemical potential for an A−B diblock chain in a cylindrical micelle within homopolymer B is

$$\frac{\mu_{mic}^{cylindrical}}{k_BT} = 1.19(\chi f_AN)^{1/3}(1.64 - \ln f_A)^{1/3} \qquad (A.14)$$

which is eq A-12 of Shull et al.[3] and eq 36 of Semenov.[29]

Lamellar Micelles. Shull et al.[3] presented the analysis for the case of lamellar micelles as well. In this case, the dimension of the core made by the A blocks is

$$R_A = Q_mf_ANb^3/A \qquad (A.15)$$

where A is the interfacial area and R_A is half the thickness of the inner lamellae. The B blocks form the corona, which extends up to distance

$$R = Q_mNb^3/A \qquad (A.16)$$

from the center of the inner lamellae. The free energy of the micelle is given by eq A.11, with the core free energy given by

$$F_{core}/kT = \frac{1.234Q_mR_A^2}{f_ANb^2} \qquad (A.17)$$

where the factor 1.234 was calculated by Semenov.[57] The free energy of the corona is given by eq A.4, with the stretching of the trajectory given by $dr(n)/dn = Q_mb^3/A$, and therefore

$$F_{corona}/kT = \frac{3}{2A^2}Q_m^2Nb^4(1 - f_A) \qquad (A.18)$$

The equilibrium value of Q_m is $Q_{m_{min}} = 0.9155A\chi^{1/6}N^{-1/3}b^{-2}(5.64 - f_A)^{-1/3}$, whereas the chemical potential for an A−B diblock chain in a lamellar micelle within homopolymer B is

$$\frac{\mu_{mic}^{lamellar}}{k_BT} = 0.669(\chi N)^{1/3}(5.64 - f_A)^{1/3} \qquad (A.19)$$

which is eq A-12 of Shull et al.[3] and somehow different from eq 36 of Semenov,[29] as also acknowledged by him.[29]

A.2. AB_2 Graft Copolymer within a B Homopolymer. Spherical Micelles. When an AB_2 graft copolymer is added to a B homopolymer, the micelles are formed with a core made up of the tooth A blocks and a corona consisting of the two B blocks. The radii R and R_A are given by eqs A.1 and A.5. The free energy of the spherical micelle is given by eq A.2, with the interfacial area $A = 4\pi R_A^2$ and the core free energy given by eq A.3. However, for the calculation of the corona free energy one has to take into account the existence of the two B blocks not only as a multiplication factor but also in modifying the stretching of the trajectory; i.e., in this

case, $dr(n)/dn = 2Q_m b^3/(4\pi r^2)$. Therefore

$$F_{corona}/kT = 2\frac{3}{2b^2}Q_m\int_{R_A}^{R} dr\,\frac{dr(n)}{dn} = 2\frac{3}{2b^2}Q_m\int_{R_A}^{R} dr\,\frac{2Q_m b^3}{4\pi r^2} \quad (A.20)$$

Thus

$$F_{corona}/kT = 2\left(\frac{3}{4\pi}\right)^{2/3} Q_m{}^{5/3} N^{-1/3}(f_A{}^{-1/3} - 1) \quad (A.21)$$

The equilibrium number of chains in the micelle is obtained as $Q_{m_{min}} = 5.1302\chi^{1/2}Nf_A{}^{2/3}(4.74f_A{}^{-1/3} - 4)^{-1}$, whereas the chemical potential for an AB_2 graft copolymer chain in a spherical micelle within homopolymer B is

$$\frac{\mu_{mic}{}^{spherical}}{k_B T} = (3/2)^{4/3} f_A{}^{4/9}(4.74f_A{}^{-1/3} - 4)^{1/3}(\chi N)^{1/3} \quad (A.22)$$

which is the same as eq 22a of Lyatskaya et al.,[22] although, in that paper, it was written that the equation is valid only for $f_A \le 0.5$.

Cylindrical Micelles. In this case, the A blocks make a core of radius R_A, given by eq A.9, whereas the B blocks form the corona, which extends up to radius R, given by eq A.10. The free energy of the micelle is given by eq A.11, with the core free energy given by eq A.12. For the calculation of the corona free energy, one uses the fact that the stretching of the trajectory is now $dr(n)/dn = 2Q_m b^3/(2\pi Lr)$ and that there are two B chains. Thus

$$F_{corona}/kT = -\frac{3}{2\pi}Q_m{}^2 bL^{-1}\ln f_A \quad (A.23)$$

The equilibrium value of Q_m is $Q_{m_{min}} = 1.32(\chi f_A N)^{1/3}(L/b)(0.41 - \ln f_A)^{-2/3}$, whereas the chemical potential for an AB_2 graft copolymer in a cylindrical micelle within homopolymer B is

$$\frac{\mu_{mic}{}^{cylindrical}}{k_B T} = 1.89(\chi f_A N)^{1/3}(0.41 - \ln f_A)^{1/3} \quad (A.24)$$

Lamellar Micelles. Here, the size of the core R_A made by the A blocks is given by eq A.15 and the size of the micelle R by eq A.16. The free energy of the micelle is given by eq A.11, with the core free energy given by eq A.17. The corona contribution again takes into account the modified stretching of the trajectory as $dr(n)/dn = 2Q_m b^3/A$ and the two B blocks. Thus

$$F_{corona}/kT = \frac{6}{A^2}Q_m{}^3 Nb^4(1 - f_A) \quad (A.25)$$

The equilibrium value of Q_m is $Q_{m_{min}} = 0.35A\chi^{1/6}N^{-1/3}b^{-2}(1.26 - f_A)^{-1/3}$, whereas the chemical potential for an AB_2 graft copolymer in a lamellar micelle within homopolymer B is

$$\frac{\mu_{mic}{}^{lamellar}}{k_B T} = 1.75(\chi N)^{1/3}(1.26 - f_A)^{1/3} \quad (A.26)$$

A.3. AB_2 Graft Copolymer within an A Homopolymer. Spherical Micelles. When an AB_2 graft copolymer is added to an A homopolymer, the micelles are formed with a core made up of the two B blocks and a corona consisting of the tooth A block. The radius of the core is

$$R_B = \left(\frac{3}{4\pi}\right)^{1/3}(Q_m[1 - f_A]Nb^3)^{1/3} \quad (A.27)$$

whereas the radius R is given by eq A.5. The free energy of the micelle is given by eq A.2, with the interfacial area $A = 4\pi R_B{}^2$. For the calculation of the core free energy, one has to take into account the existence of the two B blocks not only as a multiplication factor but also in modifying the stretching of the trajectory (another factor of 2). Thus, using eq A.3, one gets

$$F_{core}/kT = 4\left(\frac{3}{4}\right)^{5/3}\left(\frac{\pi^{4/3}}{20}\right)Q_m{}^{5/3}[(1 - f_A)N]^{-1/3} \quad (A.28)$$

The corona free energy is given by eq A.6 by replacing f_A with $1 - f_A$:

$$F_{corona}/kT = \frac{1}{2}\left(\frac{3}{4\pi}\right)^{2/3} Q_m{}^{5/3} N^{-1/3}[(1 - f_A)^{-1/3} - 1] \quad (A.29)$$

The equilibrium number of chains in the micelle is obtained as $Q_{m_{min}} = 5.1302\chi^{1/2}N(1 - f_A)^{2/3}[3.96(1 - f_A)^{-1/3} - 1]^{-1}$, whereas the chemical potential for an AB_2 graft copolymer chain in a micelle within homopolymer A is

$$\frac{\mu_{mic}{}^{spherical}}{k_B T} = (3/2)^{4/3}(1 - f_A)^{4/9}[3.96(1 - f_A)^{-1/3} - 1]^{1/3}(\chi N)^{1/3} \quad (A.30)$$

which is the same as eq 22b of Lyatskaya et al.,[22] although, in that paper, it was written that the equation is valid for an AB_2 copolymer added within a B homopolymer for $f_A \ge 0.5$. We believe that this was due to a typographical mistake.

Cylindrical Micelles. In this case, the B blocks make a core of radius R_B, given by

$$R_B = (Q_m[1 - f_A]Nb^3/(\pi L))^{1/2} \quad (A.31)$$

whereas the A blocks form the corona, which extends up to radius R, given by eq A.10. The free energy of the micelle is given by eq A.11, with the interfacial area $A = 2\pi R_B L$. For the calculation of the core free energy one has to take into account the existence of the two B blocks not only as a multiplication factor but also in modifying the stretching of the trajectory (another factor of 2). Thus, using eq A.12, one gets

$$F_{core}/kT = 4\frac{0.616Q_m R_B{}^2}{(1 - f_A)Nb^2} \quad (A.32)$$

The corona free energy is given by eq A.13 by replacing f_A with $1 - f_A$:

$$F_{corona}/kT = -\frac{3}{8\pi}Q_m{}^2 bL^{-1}\ln(1 - f_A) \quad (A.33)$$

The equilibrium value of Q_m is, thus, $Q_{m_{min}} = 3.325[\chi N(1$

$- f_A)]^{1/3}(L/b)[6.57 - \ln(1 - f_A)]^{-2/3}$, whereas the chemical potential for an AB_2 graft copolymer in a cylindrical micelle within homopolymer A is

$$\frac{\mu_{mic}^{cylindrical}}{k_B T} = 1.19[\chi(1 - f_A)N]^{1/3}[6.57 - \ln(1 - f_A)]^{1/3} \quad (A.34)$$

Lamellar Micelles. Here, the size of the core R_B made by the two B blocks is given by

$$R_B = Q_m[1 - f_A]Nb^3/A \quad (A.35)$$

and the size of the micelle R by eq A.16. The free energy of the micelle is given by eq A.11, with the corona free energy given by eq A.18 by replacing f_A with $1 - f_A$:

$$F_{corona}/kT = \frac{3}{2A^2}Q_m{}^3Nb^4f_A \quad (A.36)$$

For the calculation of the core free energy one has to take into account the existence of the two B blocks not only as a multiplication factor but also in modifying the stretching of the trajectory (another factor of 2). Thus

$$F_{core}/kT = 4\frac{1.234Q_m R_B{}^2}{(1 - f_A)Nb^2} \quad (A.37)$$

The equilibrium value of Q_m is $Q_{m_{min}} = 0.39A\chi^{1/6}N^{-1/3}b^{-2}(1.44 - f_A)^{-1/3}$, whereas the chemical potential for an AB_2 graft copolymer in a lamellar micelle within homopolymer A is

$$\frac{\mu_{mic}^{lamellar}}{k_B T} = 1.57(\chi N)^{1/3}(1.44 - f_A)^{1/3} \quad (A.38)$$

References and Notes

(1) *Polymer Blends Set: Formulation and Performance*; Paul, D. R., Bucknall, C. B., Eds.; John Wiley & Sons: New York, 2000.

(2) Fayt, R.; Jérôme, R.; Teyssié, Ph. *J. Polym. Sci., Polym. Lett. Ed.* **1986**, *24*, 25. Green, P. F.; Russell, T. P. *Macromolecules* **1991**, *24*, 2931. Dai, K. H.; Kramer, E. J. *J. Polym. Sci., Part B: Polym. Phys.* **1994**, *32*, 1943.

(3) Shull, K. R.; Kramer, E. J.; Hadziioannou, G.; Tang, W. *Macromolecules* **1990**, *23*, 4780.

(4) Russell, T. P.; Anastasiadis, S. H.; Menelle, A.; Felcher, G.; Satija, S. K. *Macromolecules* **1991**, *24*, 1575. Dai, K. H.; Norton, L. J.; Kramer, E. J. *Macromolecules* **1994**, *27*, 1949.

(5) Anastasiadis, S. H.; Gancarz, I.; Koberstein, J. T. *Macromolecules* **1989**, *22*, 1449.

(6) Wagner, M.; Wolf, B. A. *Polymer* **1993**, *34*, 1461. Jorzik, U.; Wolf, B. A. *Macromolecules* **1997**, *30*, 4713.

(7) Hu, W.; Koberstein, J. T.; Lingelser, J. P.; Gallot, Y. *Macromolecules* **1995**, *28*, 5209. Cho, D.; Hu, W.; Koberstein, J. T.; Lingelser, J. P.; Gallot, Y. *Macromolecules* **2000**, *33*, 5245.

(8) Mekhilef, N.; Favis, B. D.; Carreau, P. J. *J. Polym. Sci., Part B: Polym. Phys.* **1997**, *35*, 293. Liang, H.; Favis, B. D.; Yu, Y. S.; Eisenberg, A. *Macromolecules* **1999**, *32*, 1637.

(9) Sundararaj, U.; Macosco, C. W. *Macromolecules* **1995**, *28*, 2647.

(10) van Puyvelde, P.; Velankar, S.; Moldenaers, P. *Curr. Opin. Colloid Interface Sci.* **2001**, *6*, 457.

(11) Heikens, D.; Barentsen, W. M. *Polymer* **1977**, *18*, 70. Fayt, R.; Jérôme, R.; Teyssié, Ph. *J. Polym. Sci., Polym. Lett. Ed.* **1981**, *19*, 79. Thomas, S.; Prud'homme, R. E. *Polymer* **1992**, *33*, 4260. Tang, T.; Huang, B. *Polymer* **1994**, *35*, 281. Macosco, C. W.; Guegan, P.; Khandpur, A.; Nakayama, A.; Marechal, P.; Inoue, T. *Macromolecules* **1996**, *29*, 5590. Liang, H.; Favis, B. D.; Yu, Y. S.; Eisenberg, A. *Macromolecules* **1999**, *32*, 1637.

(12) Brown, H. *Annu. Rev. Mater. Sci.* **1991**, *21*, 463. Creton, C.; Kramer, E. J.; Hadziioannou, G. *Macromolecules* **1991**, *24*, 1846. Brown, H.; Char, K.; Deline, V. R.; Green, P. F. *Macromolecules* **1993**, *26*, 4155. Dai, C.-A.; Jandt, K. D.; Iyengar, D. R.; Slack, N. L.; Dai, K. H.; Davidson, W. B.; Kramer, E. J.; Hui, C.-Y. *Macromolecules* **1997**, *30*, 549.

(13) Noolandi, J.; Hong, K. M. *Macromolecules* **1982**, *15*, 482; **1984**, *17*, 1531. Noolandi, J. *Polym. Eng. Sci.* **1984**, *24*, 70.

(14) Duke, T. A. J. Ph.D. Dissertation, University of Cambridge, Cambridge, U.K., 1989.

(15) Fischel, L. B.; Theodorou, D. N. *J. Chem. Soc., Faraday Trans.* **1995**, *91*, 2381. Werner, A.; Schmid, F.; Binder, K.; Muller, M. *Macromolecules* **1996**, *29*, 8241.

(16) Leibler, L. *Makromol. Chem., Macromol. Symp.* **1988**, *16*, 1; *Physica A* **1991**, *172*, 258.

(17) Shull, K. R.; Kramer, E. J. *Macromolecules* **1990**, *23*, 4769.

(18) Israels, R.; Jasnow, D.; Balazs, A. C.; Guo, L.; Krausch, G.; Sokolov, J.; Rafailovich, M. *J. Chem. Phys.* **1995**, *102*, 8149.

(19) Kim, S. H.; Jo, W. H. *J. Chem. Phys.* **1999**, *110*, 12193.

(20) Vilgis, T. A.; Noolandi, J. *Makromol. Chem., Macromol. Symp.* **1988**, *16*, 225; *Macromolecules* **1990**, *23*, 2941.

(21) Gersappe, D.; Harm, P. K.; Irvine, D.; Balazs, A. C. *Macromolecules* **1994**, *27*, 720. Gersappe, D.; Balazs, A. C. *Phys. Rev. E* **1995**, *52*, 5061. Israels, R.; Foster, D. P.; Balazs, A. C. *Macromolecules* **1995**, *28*, 218. Lyatskaya, J.; Jacobson, S. H.; Balazs, A. C. *Macromolecules* **1996**, *29*, 1059. Lyatskaya, J.; Balazs, A. C. *Macromolecules* **1996**, *29*, 7581.

(22) Lyatskaya, J.; Balazs, A. C.; Gersappe, D. *Macromolecules* **1995**, *28*, 6278. Lyatskaya, J.; Gersappe, D.; Gross, N. A.; Balazs, A. C. *J. Phys. Chem.* **1996**, *100*, 1449.

(23) Dadmun, M. *Macromolecules* **1996**, *29*, 3868. Dadmun, M. *Macromolecules* **2000**, *33*, 9122.

(24) Russell, T. P.; Mayes, A. M.; Deline, V. R.; Chung, T. C. *Macromolecules* **1992**, *25*, 5783. Brown, H. R.; Krappe, U.; Stadler, R. *Macromolecules* **1996**, *29*, 6582. Guo, H. F.; Packirisamy, S.; Mani, R. S.; Aronson, C. L.; Cvozdic, N. V.; Meier, D. J. *Polymer* **1998**, *39*, 2495. Cigana, P.; Favis, B. D. *Polymer* **1998**, *39*, 3373.

(25) Tsitsilianis, C.; Voulgas, D.; Kosmas, D. *Polymer* **1998**, *39*, 3571.

(26) Dai, C.-H.; Dair, B. J.; Dai, K. H.; Ober, C. K.; Kramer, E. J. *Phys. Rev. Lett.* **1994**, *73*, 2472. Kulasekere, R.; Kaiser, H.; Ankner, J. F.; Russell, T. P.; Brown, H. R.; Hawker, C. J.; Mayes, A. M. *Macromolecules* **1996**, *29*, 5493. Smith, G. D.; Russell, T. P.; Kulasekere, R.; Ankner, J. F.; Kaiser, H. *Macromolecules* **1996**, *29*, 4120. Benkoski, J. J.; Fredrickson, G. H.; Kramer, E. J. *J. Polym. Sci., Part B: Polym. Phys.* **2001**, *39*, 2363. Eastwood, E. A.; Dadmun, M. D. *Macromolecules* **2002**, *35*, 5069.

(27) Whitmore, M. D.; Noolandi, J. *Macromolecules* **1985**, *18*, 657.

(28) Shull, K. R.; Winey, K. I.; Thomas, E. L.; Kramer, E. J. *Macromolecules* **1991**, *24*, 2748.

(29) Semenov, A. N. *Macromolecules* **1992**, *25*, 4967.

(30) Retsos, H.; Margiolaki, I.; Messaritaki, A.; Anastasiadis, S. H. *Macromolecules* **2001**, *34*, 5295.

(31) Adedeji, A.; Lyu, S.; Macosco, C. W. *Macromolecules* **2001**, *34*, 8663.

(32) Orr, C. A.; Adedeji, A.; Hirao, A.; Bates, F. S.; Macosco, C. W. *Macromolecules* **1997**, *30*, 1243. Schulze, J. S.; Cernohous, J. J.; Hirao, A.; Lodge, T. P.; Macosco, C. W. *Macromolecules* **2000**, *33*, 1191. Schulze, J. S.; Moon, B.; Lodge, T. P.; Macosco, C. W. *Macromolecules* **2001**, *34*, 200.

(33) Lee, Y.; Char, K. *Macromolecules* **1994**, *27*, 2603. Konig, C.; van Duin, M.; Pagnoulle, C.; Jérôme, R. *Prog. Polym. Sci.* **1998**, *23*, 707. Pagnoulle, C.; Konig, C.; Leemans, L.; Jérôme, R. *Macromolecules* **2000**, *33*, 6275. Pagnoulle, C.; Jérôme, R. *Macromolecules* **2001**, *34*, 965. Yin, Z.; Koolic, C.; Pagnoulle, C.; Jérôme, R. *Macromolecules* **2001**, *34*, 5132.

(34) Anastasiadis, S. H.; Chen, J.-K.; Koberstein, J. T.; Siegel, A. F.; Sohn, J. E.; Emerson, J. A. *J. Colloid Interface Sci.* **1987**, *119*, 55. Anastasiadis, S. H. Ph.D. Dissertation, Princeton University, Princeton, NJ, 1988. Anastasiadis, S. H.; Gancarz, I.; Koberstein, J. T. *Macromolecules* **1988**, *21*, 2980.

(35) Iatrou, H.; Hadjichristidis, N. *Macromolecules* **1992**, *25*, 4649. Iatrou, H.; Siakali-Kioulafa, E.; Hadjichristidis, N.; Roovers, J.; Mays J. W. *J. Polym. Sci., Part B: Polym. Phys.* **1995**, *33*, 1925.

(36) Pochan, D. J.; Gido, S. P.; Pispas, S.; Mays, J. W.; Ryan, A. J.; Fairclough, J. P. A.; Hamley, I. W.; Terrill, N. J. *Macromolecules* **1996**, *29*, 5091. Pochan, D. J.; Gido, S. P.; Pispas, S.; Mays, J. W. *Macromolecules* **1996**, *29*, 5099. Anastasiadis, S. H.; Chrissopoulou, K.; Fytas, G.; Fleischer, G.; Pispas, S.; Pitsikalis, M.; Mays, J. W.; Hadjichristidis, N. *Macromolecules* **1997**, *30*, 2445.

(37) Pispas, S.; Hadjichristidis, N.; Potemkin, I.; Khokhlov, A. *Macromolecules* **2000**, *33*, 1741.

(38) Hadjichristidis, N.; Iatrou, H.; Pispas, S.; Pitsikalis, M. *J. Polym. Sci., Part A: Polym. Chem.* **2001**, *38*, 3211.
(39) Xing, P.; Bousmina, M.; Rodrigue, D.; Kamal, M. R. *Macromolecules* **2000**, *33*, 8034.
(40) Bashforth, S.; Adams, J. C. *An Attempt to Test the Theory of Capillary Action*; Cambridge University Press and Deighton, Bell & Co.: London, 1882.
(41) The instrument described in ref 31 has been commercialized by Materials Interface Associates.
(42) Richardson, M. J.; Savill, N. G. *Polymer* **1977**, *18*, 3.
(43) Han, C. D.; Kim, J.; Kim, J. K. *Macromolecules* **1989**, *22*, 383.
(44) Strobl, G. R. *Acta Crystallogr., Sect. A* **1970**, *A26*, 367.
(45) Rigby, D.; Roe, R.-J. *Macromolecules* **1984**, *17*, 1778; **1986**, *19*, 721. Roe, R.-J. *Macromolecules* **1986**, *19*, 728. Nojima, S.; Roe, R.-J.; Rigby, D.; Han, C. C. *Macromolecules* **1990**, *23*, 4305.
(46) Since the aim of the present work was not to investigate the concentration dependence in any more detail, data points at very low concentrations were not measured for these and other copolymers, and therefore, the concentration required to achieve 1/*e* of the maximum reduction in the interfacial tension from the value in the absence of copolymer ($\gamma_0 = 1.68 \pm 0.02$ dyn/cm) to that at saturation cannot be estimated with reasonable accuracy. This reduction is usually analyzed with the equation[6,11d,30] $\gamma = (\gamma_0 - \gamma_{sat}) \exp(-w_{add}/w_{char}) + \gamma_{sat}$, where w_{char} denotes the concentration required to achieve 1/*e* of the maximum reduction $\gamma_0 - \gamma_{sat}$.
(47) Gia, H.-B.; Jérôme, R.; Teyssié, Ph. *J. Polym. Sci., Polym. Phys. Ed.* **1980**, *18*, 2391.
(48) Welge, I.; Wolf, B. A. *Polymer* **2001**, *42*, 3467.
(49) It is believed that this finding is more general since in every case when mixtures of additives (either linear diblocks or grafts) were investigated by us, the obtained interfacial tension was that of the lowest of the two values obtained by the individual additives alone. It is planned to further investigate whether this occurs even for concentrations lower than those at saturation.
(50) Porod, G. *Kolloid-Z.* **1951**, *124*, 83; **1952**, *125*, 51; **1952**, *125*, 103.
(51) Guinier, A.; Fournet, G. *Small-angle Scattering of X-rays*; John Wiley: New York, 1955.
(52) Koberstein, J. T.; Morra, B.; Stein, R. S. *J. Appl. Crystallogr.* **1979**, *12*, 330.
(53) Helfand, E.; Tagami, Y. *J. Chem. Phys.* **1971**, *56*, 3592; **1972**, *57*, 1812.
(54) de Gennes, P. G. *Macromolecules* **1980**, *13*, 1069.
(55) It is noted that Noolandi[56] objects the use of eqs 5 and 9 since he claims that the main contribution to the interfacial tension reduction is of enthalpic and not entropic origin (as eq 9 suggests), i.e., that it is due to the favor energetics of the orientation of the copolymer blocks into their respective homopolymers and that entropic effects are second order. He suggests that eq 9 should be corrected by adding the contributions of the orientational entropy of the blocks and their entropy of localization; the latter was introduced by Shull and Kramer[17] by replacing γ_0 by $\gamma_0' = \gamma_0 + \sigma k_B T \ln[(L_A + L_B)/d']$. In the present analysis, the Leibler[2b,16] expression is utilized.
(56) Noolandi, J. *Makromol. Chem., Rapid Commun.* **1991**, *12*, 517.
(57) Semenov, A. N. *Zh. Eksp. Teor. Fiz.* **1985**, *88*, 1242; *Sov. Phys. JETP* **1985**, *61*, 733.

MA035463E